Interaction of proteinase inhibitors with phospholipid vesicles is modulated by pH

ARTICLE *in* INTERNATIONAL JOURNAL OF BIOLOGICAL MACROMOLECULES · NOVEMBER 2010

Impact Factor: 2.86 · DOI: 10.1016/j.ijbiomac.2010.07.011 · Source: PubMed

7 AUTHORS, INCLUDING:

Rosemeire Lucca
Universidade Estadual Do Oeste Do Parana
17 PUBLICATIONS **139** CITATIONS
SEE PROFILE

Henrique Faneca
Center for Neurosciences and cell biology, …
42 PUBLICATIONS **908** CITATIONS
SEE PROFILE

Misako U Sampaio
Universidade Federal de São Paulo
95 PUBLICATIONS **1,277** CITATIONS
SEE PROFILE

Maria Luiza V Oliva
Universidade Federal de São Paulo
85 PUBLICATIONS **1,100** CITATIONS
SEE PROFILE

International Journal of Biological Macromolecules 47 (2010) 551–557

Contents lists available at ScienceDirect

International Journal of Biological Macromolecules

journal homepage: www.elsevier.com/locate/ijbiomac

Interaction of proteinase inhibitors with phospholipid vesicles is modulated by pH

Rosemeire A. Silva-Lucca[a,b], Henrique M.S. Faneca[c], Maria C. Pedroso de Lima[c], Fernanda P. De Caroli[a], M.L. Assis[a], Misako U. Sampaio[a], Maria Luiza V. Oliva[a,*]

[a] Departamento de Bioquímica, Universidade Federal de São Paulo-Escola Paulista de Medicina, Rua Três de Maio, 100 Vila Clementino, 04044-020 São Paulo, SP, Brazil
[b] Centro de Engenharias e Ciências Exatas, Universidade Estadual do Oeste do Paraná-Rua da Faculdade 650, CEP 85903-000 Toledo, PR, Brazil
[c] Departamento de Ciências da Vida, Centro de Neurociências e Biologia Celular, Faculdade de Ciências e Tecnologia, Universidade de Coimbra, Apartado 3126, 3001-401, Coimbra, Portugal

ARTICLE INFO

Article history:
Received 8 March 2010
Received in revised form 5 July 2010
Accepted 28 July 2010
Available online 6 August 2010

Keywords:
Bauhinia
Circular dichroism
Fluorescence spectroscopy
Liposome
Plant proteinase inhibitors
Phospholipid
Trypsin inhibitor

ABSTRACT

rBbKI and rBbCI, plant recombinant inhibitors from *Bauhinia bauhinioides*, and BpuTI from *Bauhinia purpurea* seeds distinctly and specifically block proteolytic enzymes. The secondary structures of those inhibitors were compared and their interactions with phospholipid vesicles were evaluated by the release of calcein and by intrinsic fluorescence of tryptophan residues. The results show that rBbKI, rBbCI and BpuTI are able to interact with phospholipd vesicles and induce membrane permeabilization in a concentration- and pH-dependent manner. The leakage was rapid and extensive at pH 4.5, but at physiological pH, no calcein release was observed. These results may suggest that upon inflammation or microorganism invasion accompanied by lowering of pH, appropriate conditions may occur for the inhibitors to interact with cell membrane and act on specific proteolytic enzyme.

1. Introduction

Kunitz-type inhibitors constitute a large and well-characterized plant protein family, which is probably due to their relatively abundant distribution in most plant organs, mainly in the legume [1]. Due to their actions on target enzymes in a diverse array of biological processes, these proteins are useful tools for the investigation of digestion [2,3], coagulation [4,5], inflammation [6,7], cancer [8–10] and fibrinolysis [11,12]. All of these events involve a complex meshwork of activities. This includes serine and metalloproteinase (MMP) enzymes, which are active mostly at neutral pH and are responsible for extracellular proteolysis, and aspartyl and cysteine enzymes, which function at low pH and are involved mainly in intracellular proteolysis within lysosomes [13,14].

Among the lysosomal cysteine proteinases, cathepsin B and L have been the most extensively investigated due to their role in processes such as cancer progression [15–19]. Besides differences in cell compartmentalization, their action is accomplished by a cooperative interaction between several proteinases leading to a proteolytic net activation. For example, most MMP activation is initiated in the extracellular space by serine proteinases such as plasmin and urokinase plasminogen activator, neutrophil elastase or by other members of the MMP family, especially MMP-2 and MMP-13, by MT1-MMP cleavage of the proenzymes [13,20]. Procathepsin B can be activated by cathepsin D, elastase and cathepsins G, uPA or tPA [21].

Under physiological conditions, equilibrium between proteinases and their inhibitors exists in the organism. However, under pathological conditions, such as oxidative stress observed in tumor development or inflammation, an imbalance of the proteolytic–antiproteolytic system may lead to enhanced proteolysis [22]. Thus, functional development of more specific proteinase inhibitors may lead to novel compounds to block proteinase activity.

Many proposed functions of the inhibitory proteins depend on their ability to bind to the cell surface, and since biological membranes are negatively charged, we studied the interaction of plant proteinase inhibitors with vesicles made from negatively charged phospholipids with the aim of understanding the inhibitory activity and mechanisms of action.

* Corresponding author. Tel.: +55 11 5576 4444; fax: +55 11 5572 3006.
E-mail address: olivaml.bioq@epm.br (M.L.V. Oliva).

0141-8130/$ – see front matter © 2010 Elsevier B.V. All rights reserved.
doi:10.1016/j.ijbiomac.2010.07.011

2. Materials and methods

2.1. Materials

Enzymes. Human plasma kallikrein (HuPK) (EC 3.4.21.34) was purified by a previously described procedure [23]. Bovine trypsin (EC 3.4.21.4) was from Sigma (St. Louis, USA) and porcine pancreatic elastase (PPE) (EC 3.4.21.36) was obtained from Calbiochem Ltd. (San Diego, USA).

Substrates. p-Nitroanilide (pNa), Bz-Arg-pNa; H-Pro-Phe-Arg-MCA, Ac-Phe-Arg-pNa and MeO-Suc-Ala-Ala-Pro-Val-pNa were from Calbiochem Ltd. (San Diego, USA).

2.2. Inhibition assay

The inhibitory activity towards trypsin, pancreatic elastase, and plasma kallikrein was assayed as described previously [24–26]. Trypsin active site concentration was determined by NPGB titration [27] and BpuT concentration was determined by titration with trypsin assuming an equimolar binding between the enzyme and the inhibitor. The concentration of the recombinant proteins was estimated using the extinction coefficient at 280 nm as 0.847 M^{-1} cm^{-1} calculated using ExPASy (Expert Protein Analysis System) [28]. The pH effect on inhibitor activity was determined through pre-incubation for 10 min at 37 °C in buffers with pH values ranging from 2.0 to 8.0. The pH was subsequently adjusted to 8.0, and the specific enzyme inhibition of trypsin by BbKI and BpuTI was assayed at 1.0 mM DL-Bz-Arg-pNa and of pancreatic elastase by BbCI using 0.5 mM MeO-Suc-Ala-Ala-Pro-Val-pNa as a substrate.

2.3. Circular dichroism measurements

Far UV CD spectra (190–250 nm) were recorded at room temperature (25 °C) on a Jasco J-810 spectropolarimeter using a 1 mm path length cell and each spectrum was recorded as an average of eight scans. The instrument was calibrated with a 0.1% d-10-camphorsulfonic acid solution. Ellipticity is reported as the mean residue ellipticity, $[\theta]$ (deg cm^2 $dmol^{-1}$), defined as:

$$[\theta] = \frac{\theta_{obs}}{10lCN}$$

where θ_{obs} is the observed ellipticity in degrees, l is the path length in centimeters, C is the molar concentration and N is the number of amino acid residues. The control baseline was obtained with buffer and all the components without proteins. The secondary structure estimate was performed using the CDPro software package [29] that provides three programs for estimation of secondary structure fractions from CD spectra: SELCON 3, CONTIN/LL and CDSSR. The analysis with all the programs improves the reliability of the secondary structure predictions with a root mean square (RMS) lower than 3% for all deconvolutions.

2.4. Fluorescence measurements

Fluorescence measurements were performed at 25 °C. Samples were excited at 280 or 295 nm and the emission was monitored in the range 290–450 nm or 305–450 nm. Quartz cuvettes with a 1 cm path length were used for all the measurements. The protein concentration used in these experiments was approximately 0.09 mg/ml so that the optical density at 280 nm was always less than 0.1. Fluorescence spectra were recorded at various pH values in the range 2.0–12.0, in 10 mM acetate/borate/phosphate buffer.

2.5. Preparation of phospholipid vesicles

Egg L-α-phosphatidic acid (PA) and egg L-α-phosphatidylethanolamine (PE) were purchased from Avanti Polar Lipids. Dried lipid films were hydrated by extensive vortexing in 10 mM HEPES, 140 mM NaCl, pH 7.4, for tryptophan fluorescence measurements, or in 15 mM calcein (Sigma), 10 mM HEPES, 140 mM NaCl, pH 7.4 for the leakage assays. Large unilamellar vesicles were prepared by extrusion of these multilamellar liposomes through two stacked polycarbonate filters (pore size 0.1 μm). Free calcein was separated from the dye-containing LUV by size exclusion chromatography on a Sephadex G-75 column. Phospholipid concentration (2.2 mM) was measured by the Fiske and Subbarow method [30]. The lipid composition of the vesicles had a molar ratio PA:PE (1:1).

2.6. Leakage assays

The leakage of liposome (8 μM) content was monitored by the release of calcein encapsulated at a self-quenching concentration. The leakage experiments were carried out at 37 °C and fluorescence measurements were performed in a Hitachi 2900 spectrofluorometer equipped with a constant-temperature cell holder and stirrer, in 10 mM HEPES, 140 mM NaCl, pH 4.5–7.4. After protein addition (0.1–1.0 μM) the leakage of calcein into the external medium was monitored by the increase in fluorescence caused by the reduction in self-quenching upon calcein dilution (excitation 494 nm, 517 nm emission, slit width 0.5). Baseline fluorescence (0%) was determined before protein addition and complete leakage (100%) was established following the liposome lysis assays monitored with extran. In the beginning of all experiments, the control performed to verify the encapsulation of calcein, which is related to phospholipid vesicles stability, showed no variation in the residual leakage. The results represent the mean of three experiments.

2.7. Tryptophan fluorescence and CD spectra measurements of inhibitors with LUVs

The intrinsic fluorescence of the tryptophan residues of the inhibitors (1.0 μM) was measured at 37 °C in 10 mM HEPES, 140 mM NaCl, pH 4.5 (maximal leakage) and 7.4 (minimal leakage). The excitation of inhibitor samples was performed at 295 nm, where emission is only due to the tryptophan residues and tyrosine is neither excited nor emits at this wavelength. The emission spectra were recorded from 305 to 420 nm in the presence and the absence of LUVs (8 μM). The spectra were corrected for the intrinsic fluorescence of buffer and phospholipids. The CD spectra of inhibitors (1.0 μM) were recorded over a wavelength range of 190–250 nm, at 37 °C, in 10 mM HEPES, 140 mM NaCl, pH 4.5 (maximal leakage) in the absence or in the presence of LUVs. All CD spectra measured were baseline corrected by the buffer or the buffer and phospholipids.

3. Results and discussion

3.1. Effect of temperature and pH on inhibitor activity

Bauhinia plant Kunitz-type inhibitors named BbCI (*B. bauhinioides* cruzipain inhibitor), BbKI (*B. bauhinioides* kallikrein inhibitor) and BpuTI (*B. purpurea* trypsin inhibitor) are 18–20 kDa proteins that are similar to most Kunitz-type proteinase inhibitors. BpuTI is similar to classical Kunitz-type inhibitors bearing two disulfide bridges, in contrast to rBbCI and rBbKI, which are devoid of disulfide bridges [24–26,31]. Concerning the specificity, BbCI efficiently inhibits the cysteine proteinase cruzipain (0.30 nM) and cathepsin L (22 nM) but not human cathepsins B, K, X, V, or the

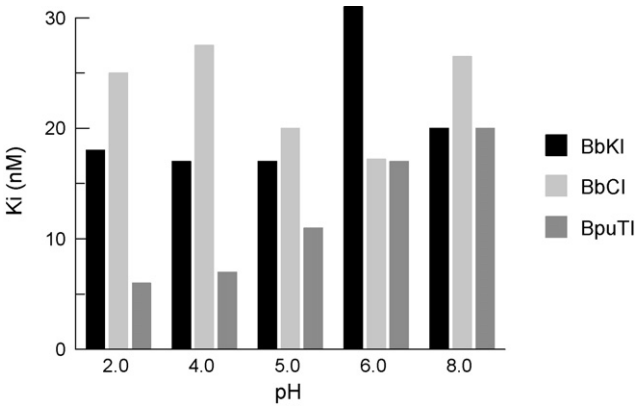

Fig. 1. Effect of pH on inhibitor activity. The pH effect on inhibitor activity was determined through pre-incubation for 10 min at 37 °C in buffers with pH values ranging from 2.0 to 8.0. The residual inhibitory activity assayed on trypsin (7.0 nM in 0.05 M Tris/HCl, pH 8.0, 0.02% $CaCl_2$; 1.0 mM Bz-Arg-pNa) was determined with BbKI and BpuTI and on PPE, porcine pancreatic elastase (24 nM in 0.05 M Tris/HCl, pH 8.0, 0.5 M NaCl; 0.5 mM MeO-Suc-Ala-Ala-Pro-Val-pNa) with BbCI. K_{iapp} values were determined by adjusting the experimental points to the equation for tight binding using a non-linear regression with the Grafit program (Morrison, 1982).

plant cysteine proteinases bromelain, papain and ficin. BbCI also inhibits the serine proteinases cathepsin G (K_{iapp} 160 nM), human neutrophil elastase (K_{iapp} 5.3 nM) and porcine pancreatic elastase (K_{iapp} 40 nM). No effect was observed on blood clotting enzymes [6,24,31]. The same species *bauhinioides* also produces BbKI with a high primary structural identity (81%) to BbCI. However, despite of the structural similarity, they differ on the inhibitory specificity. BbKI inhibits kallikrein (human plasma and tissue), plasmin and trypsin, while BbCI does not interfere on the activity of these enzymes [25,31]. In a previous work, recombinant rBbKI and rBbCI were reported to exhibit the same properties as the native forms [26]. In this study, we evaluated the effect of temperature and pH stability on those inhibitors using some model enzymes such as trypsin for rBbKI and BpuTI and elastase for rBbCI.

Although a decrease in the numerical values of the apparent K_i (K_{iapp}) was observed for trypsin inhibition by pre-incubation for 10 min with BpuTI and rBbKI, in the pH range 2.0–8.0, and for BbCI on human neutrophil elastase (Fig. 1), the values are in the same order of magnitude, suggesting that these proteins can act in acidic environment, as occurs in pathological conditions.

3.2. Effect of pH on secondary structure

Circular dichroism (CD) was used to follow changes in secondary structure of the interacting proteins. The CD spectrum of BpuTI at pH 7.4, 25 °C (Fig. 2A) exhibits one pronounced negative peak at 200 nm and a positive peak at 230 nm, which is comparable to that of soybean trypsin inhibitor (SBTI).

Positive and negative bands in the region of 200 nm usually represent β-sheet and unordered structures, respectively. However, by using the cluster analysis it was possible to verify that those proteins belong to the second set of rich-β proteins, termed β-II proteins, which are similar to soybean trypsin inhibitor [32,33].

BbCI and BbKI contain 9 and 3 tyrosine residues, respectively, and 8 residues of phenylalanine and one tryptophan residue each. Aromatic residues represent approximately 10% of the BbKI and 8% of the BbCI polypeptide chains.

The positive band near 230 nm usually indicates the interference of aromatic amino acid groups or the presence of disulfide bridges [34,35]. As it was reported rBbCI and rBbKI do not contain disulfide bridges [24–26,31], this band indicates the contribution of aromatic residues, while in BpuTI that band could be the result

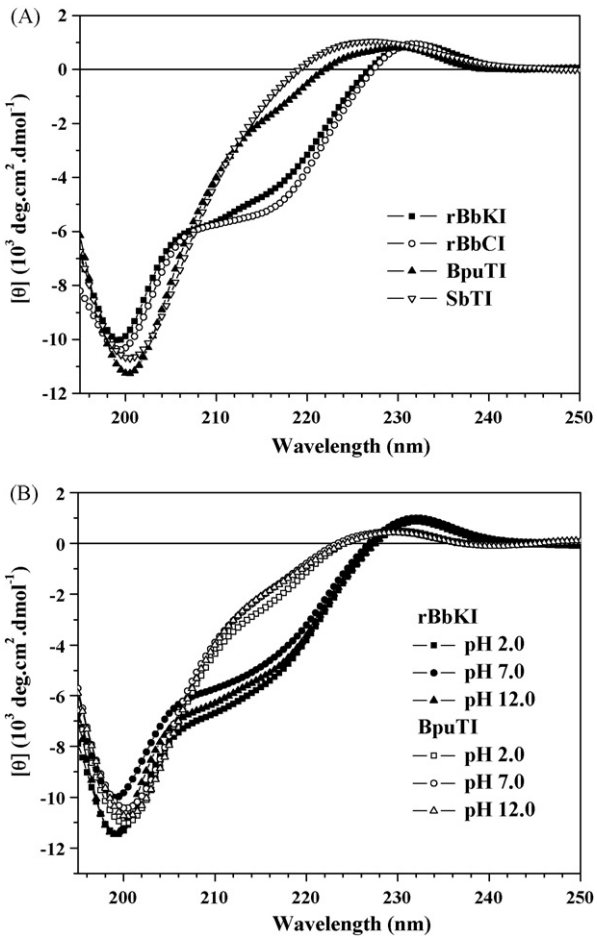

Fig. 2. (A) CD spectra of inhibitors in 10 mM phosphate buffer, pH 7.4. Measurements were recorded as an average of 8 scans for protein solutions of 0.18 mg/ml at 25 °C. (B) CD spectra of inhibitors as a function of pH. The samples were incubated in 10 mM acetate/borate/phosphate buffer, pH 2–12 for 15 min prior to the spectrum measurement.

of both aromatic residues and disulfide bridges. These results indicate that changes in CD spectra in this region are not due to the disulfide bridges. The CD spectra of rBbKI and rBbCI showed a band at 216 nm besides those observed in the spectra of BpuTI and SBTI. In addition, such spectra are the same of the native proteins, being an additional tool for monitoring the folding of the recombinant forms.

No significant differences were observed in the estimate of their secondary structures, in comparison to BpuTI and SbTI, which are used as the model of the classical two disulfide-bridges plant-Kunitz inhibitors (Table 1). rBbKI and rBbCI typical spectra might be considered a model for characterization of new members of Kunitz inhibitors devoid of cysteine residues or disulfide bridges.

No significant changes due to pH were observed in rBbKI and BpuTI CD spectra (Fig. 2B), showing that the secondary structures of those inhibitors are not altered in acidic or basic pH conditions.

Table 1
Secondary structure of inhibitors estimated from CD spectra.

Protein	α-Helix (%)	β-Sheet (%)	β-Turn	Unordered (%)
rBbKI	4	39	21	32
rBbCI	4	42	22	30
BpuTI	6	40	22	30
SBTI	2	36	23	37

Quantitative predictions were performed using CDPro software with RMS lower than 3% for all deconvolutions.

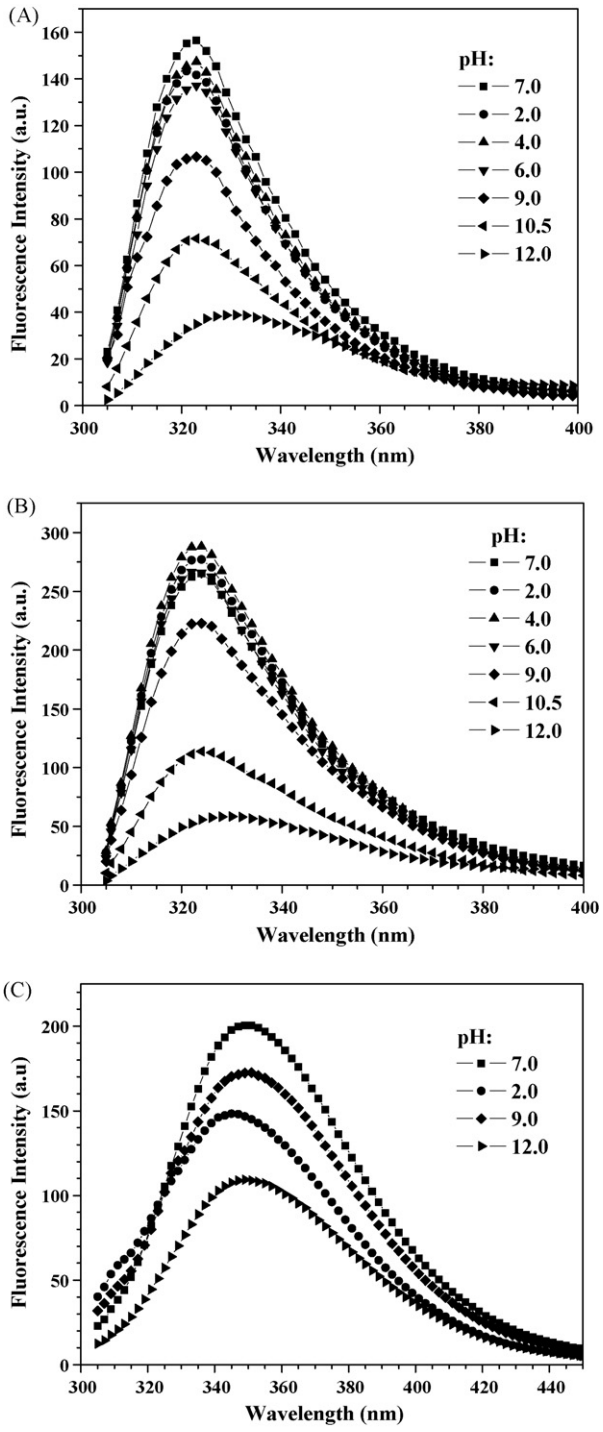

Fig. 3. Fluorescence emission spectra of (A) rBbCI, (B) rBbKI and (C) BpuTI as a function of pH. Fluorescence spectra were recorded at various pH values in the range 2.2–12.0 in 10 mM acetate/borate/phosphate buffer.

rBbCI spectra were identical to those of rBbKI. This stability indicates that these proteins exhibit a pH conformational resistance, which is important for maintenance of protein functionality under pathological circumstances in which pH is altered.

3.3. Fluorescence spectra of inhibitors in acidic and basic pH conditions

The fluorescence spectra of rBbCI and rBbKI show difference in the intensity (Fig. 3A and B), although the emission maxima

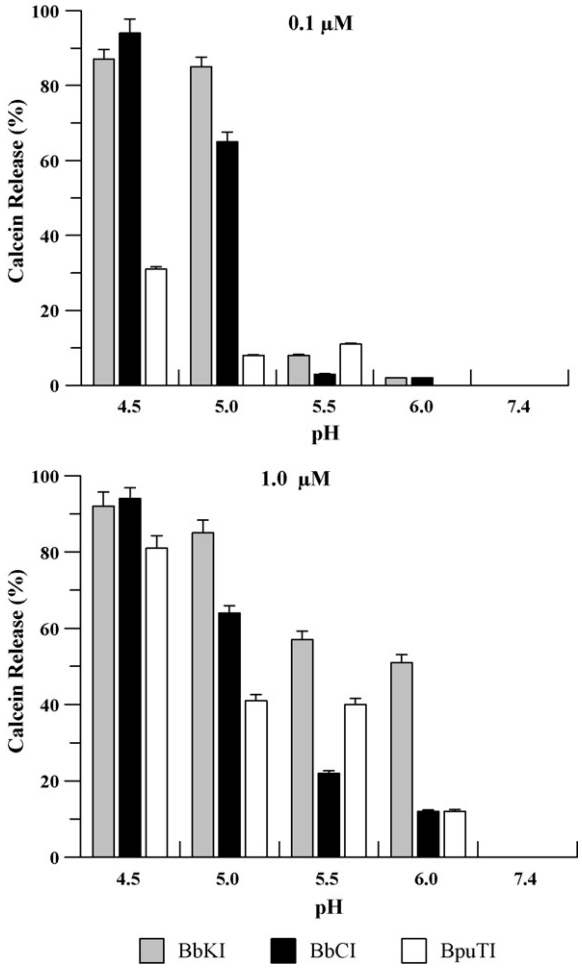

Fig. 4. Effect of inhibitor concentration on calcein release at different pH values. BbKI (gray), BbCI (black), and BpuTI (white) in concentrations of 0.1 and 1.0 μM were incubated with PA/PE (1:1) (8 μM) containing calcein for 10 min at 37 °C in 10 mM HEPES solution, 0.14 M NaCl, pH 4.5, 5.0, 5.5, 6.0 and 7.4. Each data position is an average of three experiments and error bars show the standard deviation.

(323 nm) of both inhibitors are the same in the pH range 2.0–10.5, suggesting that these structures are steady when exposed to pHs different from the usual for its inhibitory activity (ca. 8.0).

The fluorescence intensity of both inhibitors showed small variations under acid conditions, in contrast to their spectra in basic conditions where the intensity decreased around 55%, at pH 10.5 and more than 75%, at pH 12.0. These fluorescence quenching may be explained by occurrence of the nonradiative pathways including the presence of Lys (pKa = 10.7) and Arg (pKa = 12) residues in the proximity of Trp residues (<8 Å), as seen in the three-dimensional structures of rBbCI and rBbKI [36,37], probably leading to excited-state proton transfer reactions [38–40]. The red-shift (323–330 nm) at pH 12.0 indicates that tryptophan becomes more exposed to a polar environment.

The fluorescence spectrum of BpuTI is characteristic of tryptophan totally exposed to solvent, with an emission maximum at 350 nm, at pH 7.0 (Fig. 3C) that altered only at pH 2.0 with a small blue-shift to 346 nm. In this case, decrease of fluorescence intensity is observed at acidic and basic pHs suggesting the presence of ionized acid and basic amino acids in the neighboring of Trp.

The intrinsic fluorescence of tyrosine residues was not directly detected in the spectra at 280 nm excitation because no modification in the maximum of emission and the shape of the spectra was observed (data not shown), in comparison to what is observed at 295 nm excitation. A significant increase in the fluorescence inten-

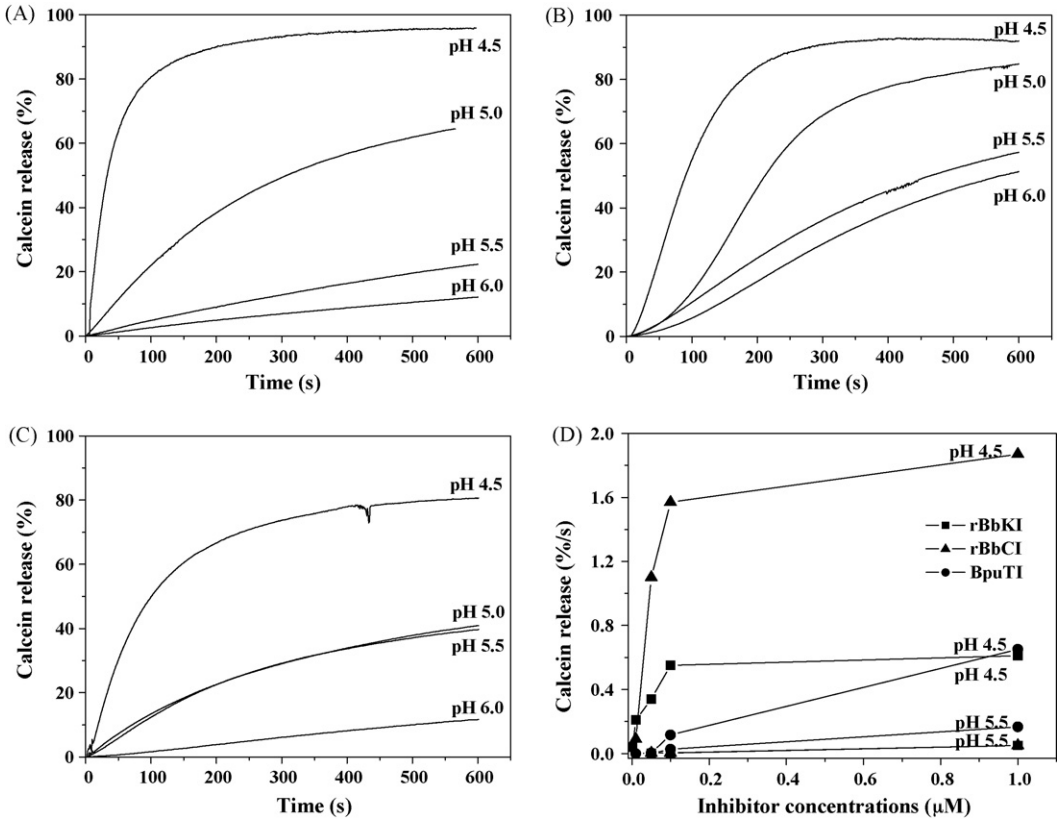

Fig. 5. pH dependence on *Bauhinia* inhibitor-induced vesicle leakage. LUV (8 μM) with entrapped calcein composed of PA/PE (1:1) were incubated with 1 μM of (A) BbCI, (B) BbKI and (C) BpuTI in a final volume of 2 mL at 37 °C in a stirred cuvette. The release of calcein was monitored for 10 min in 10 mM HEPES solution, 0.14 M NaCl at pH 4.5, 5.0, 5.5, 6.0 and 7.4. Each curve is the average of three experiments. (D) Effect of inhibitor concentration and pH on the initial rate of calcein release. Inhibitors were incubated with PA/PE (1:1) (8 μM) containing calcein for 10 min at 37 °C. The initial rate of release was determined from the tangents at $t = 0$ to curves such as those presented in (A)–(C) and plotted as a function of inhibitor concentration. The data points represent the mean of three experiments.

sity is observed because, at 280 nm, the fluorophores have a higher quantum yield and a transfer of energy from tyrosine to tryptophan residues occurs.

3.4. Interaction of Bauhinia inhibitor with phospholipid vesicles

To gain a better insight into the properties and functionality of the studied inhibitors, we investigated their interaction on negatively charged liposomes that mimic cell membranes as a function of pH (4.5–7.4) and protein concentration (0.001–1.0 μM). The overall effect of pH and concentration (0.1 and 1.0 μM) on calcein release by inhibitors is shown in Fig. 4. The leakage induced by inhibitors was found to be concentration and pH-dependent for the phospholipid vesicle composition tested. The effect of rBbCI and rBbKI on calcein release is more efficient than that of BpuTI because only at 1.0 μM concentration is the leakage of vesicles by BpuTI comparable to that of rBbKI and rBbCI, mainly at pH 4.5–5.0. At pH 7.4 no calcein release was detected, but as the pH became more acidic, both the initial rates and extent of leakage increased, being most efficient at pH 4.5. In the case of rBbKI, the acidic condition is not as critical as it is for rBbCI and BpuTI. For example, at pH 6.0, the calcein release reached 10% for rBbCI and BpuTI, while the release by rBbKI was 55% (Fig. 4). This observation suggests that the inhibitors would interact differently with cells under acidic pathological conditions.

At pH 4.5 and 1.0 μM inhibitor, the velocity of calcein release by rBbCI is faster than that of rBbKI and BpuTI, as seen by the slope of the release curve (Fig. 5A–C). Seventy percent of leakage was achieved by rBbCI within the first 60 s (Fig. 5A), while this level of leakage by rBbKI (Fig. 5B) and BpuTI (Fig. 5C) takes place only after 135 and 240 s, respectively. Furthermore, the efficiency of encapsulated calcein release in the presence of rBbCI and rBbKI are similar, leading to a maximum of ~90% at 100 s, while within this period BpuTI reached 80%.

The influence of pH and concentration on the initial velocity of calcein release was also correlated (Fig. 5D). Rates were determined by the tangent to the curves (Fig. 5A–C) at $t = 0$. In the range of protein concentrations that we used, the release of calcein showed a non-linear dependence with concentration (Fig. 5D). The release of calcein is fast and efficient when induced by inhibitors, but it occurs with different kinetics, as shown by the difference between the initial velocities of probe release induced by them. At 0.1 μM and pH 4.5, the initial leakage rate is higher for rBbCI (1.6%/s), followed by BbKI (0.5%/s) and BpuTI (0.1%/s). The parameters are the same in the case of 1 μM rBbCI. However, the lack of variation between rBbKI and BpuTI indicates that, although the initial velocities of rBbKI and BpuTI are different, they are no longer significant at 1 μM. On the other hand, the velocity and the efficiency of calcein release of all inhibitors are disrupted at pH 5.5 independent of applied concentration.

To further investigate the interaction of the inhibitors with phospholipid vesicles, the intrinsic fluorescence of tryptophan residues of the inhibitors was measured in the presence and absence of LUVs (PA:PE) at pH 4.5 (maximal leakage) and pH 7.4 (minimal leakage). The fluorescence emission maxima of tryptophan residues of rBbKI and rBbCI remained unchanged in the presence of phospholipid vesicles at pH 4.5 and 7.4 (data not shown). Similarly, the fluorescence maximum of BpuTI at pH 7.4 remains unchanged in the presence of LUVs at 350 nm, consistent with tryptophan residues totally exposed to solvent. Moreover,

at pH 4.5, there was a blue-shift of the emission maximum to 342 nm, compatible with the change of tryptophan residues to a more hydrophobic microenvironment, which is probably due to its insertion into the membrane of the vesicles (data not shown). This shift was not observed for the maximum emission of inhibitors rBbKI and rBbCI, which is probably because tryptophan residues already were in a hydrophobic microenvironment.

In addition, possible changes in the secondary structure of the inhibitors under interaction with membrane vesicles were monitored by CD spectra in the absence and in the presence of LUVs. There were no changes in the CD spectra of the inhibitors when interacting with phospholipid vesicles (data not shown).

4. Conclusions

In conclusion, using both the conformational information of native or recombinant proteinase inhibitors in solution and the interaction with phospholipid vesicles as a model system, we have been able to demonstrate that the studied proteins adopt a conservative conformational state that persists at different pH conditions. The reported findings also provide clear evidence for the occurrence of pH-induced electrostatic interactions with phospholipid vesicles and point to *Bauhinia* inhibitors as valuable tools for the understanding of diverse mechanisms, which correlate their biological properties of inhibiting proteinase activity. For example, since BbCI is known to inhibit specifically a lysosomal cathepsin L enzyme at pH 4.5, our results suggest that, under acid pH conditions, the inhibitors may interact with cell membrane and are still able to inhibit uncontrolled proteolysis (showed by its functional and structural stability), as it occurs with kininogens, the major plasma cystatin-like inhibitor, which bind to the cell membrane, mediated by different structures, internalizes and act on cysteine cathepsin [41–43]. These findings may help to clarify the action of similar plant inhibitors on biological models, and pH-induced conformational changes, to understand some functional aspects of the protein *in vivo*, particularly under pathological conditions, connected with local fluctuations of pH.

Conflict of interest statement

The authors have declared that no conflict of interest exists.

Acknowledgments

This work was partially supported by CAPES/DAAD/Grices, CNPq, and FAPESP.

References

[1] Y. Birk, Plant Protease Inhibitors: Significance in Nutrition, Plant Protection, Cancer Prevention and Genetic Engineering, Springer-Verlag, Berlin Heidelberg, 2003.
[2] M.L.R. Macedo, M.G.F. Freire, E.C. Cabrini, M.H. Toyama, J.C. Novello, S. Marangoni, A trypsin inhibitor from *Peltophorum dubium* seeds active against pest proteases and its effect on the survival of *Anagasta kuehniella* (*Lepidoptera*: *Pyralidae*), Biochim. Biophys. Acta 1621 (2003) 170–182.
[3] H. Liao, W. Ren, Z. Kang, J.H. Jiang, X.J. Zhao, L.F. Du, A trypsin inhibitor from *Cassia obtusifolia* seeds: isolation, characterization and activity against *Pieris rapae*, Biotechnol. Lett. 29 (2007) 653–658.
[4] M.L. Oliva, S.A. Andrade, M.A. Juliano, R.C. Sallai, R.J. Torquato, M.U. Sampaio, V.J. Pott, C.A. Sampaio, Kinetic characterization of factor Xa binding using a quenched fluorescent substrate based on the reactive site of factor Xa inhibitor from *Bauhinia ungulata* seeds, Curr. Med. Chem. 10 (2003) 1085–1093.
[5] S. Macedo-Ribeiro, C. Almeida, B.M. Calisto, T. Friedrich, R. Mentele, J. Stürzebecher, P. Fuentes-Prior, P.J. Pereira, Isolation, cloning and structural characterisation of boophilin, a multifunctional Kunitz-type proteinase inhibitor from the cattle tick, PLoS One 3 (2008) 1624.
[6] C. Neuhof, M.L. Oliva, D. Maybauer, M. Maybauer, C. Oliveira, M.U. Sampaio, C.A. Sampaio, H. Neuhof, Effect of plant Kunitz inhibitors from *Bauhinia bauhinioides* and *Bauhinia rufa* on pulmonary edema caused by activated neutrophils, Biol. Chem. 384 (2003) 939–944.
[7] G.C. Mello, I.A. Desouza, N.S. Mariano, T. Ferreira, M.L. Macedo, E. Antunes, Mechanisms involved in the rat peritoneal leukocyte migration induced by a Kunitz-type inhibitor isolated from *Dimorphandra mollis* at acid and basic pHs seeds, Toxicon 53 (2009) 323–329.
[8] H. Kobayashi, M. Suzuki, N. Kanayama, T. Terao, A soybean Kunitz trypsin inhibitor suppresses ovarian cancer cell invasion by blocking urokinase upregulation, Clin. Exp. Metastasis 21 (2004) 159–166.
[9] A.M. Nakahata, N.R. Bueno, H.A. Rocha, C.R. Franco, R. Chammas, C.R. Nakaie, M.G. Jasiulionis, H.B. Nader, L.A. Santana, M.U. Sampaio, M.L. Oliva, Structural and inhibitory properties of a plant proteinase inhibitor containing the RGD motif, Int. J. Biol. Macromol. 40 (2006) 22–29.
[10] X. Ye, T.N. Bun, A trypsin–chymotrypsin inhibitor with antiproliferative activity from small glossy black soybeans, Planta Med. 75 (2009) 550–556.
[11] M.L.V. Oliva, J.C. Souza-Pinto, I.F.C. Batista, M.S. Araujo, V.F. Silveira, E.A. Auerswald, R. Mentele, C. Eckerskorn, M.U. Sampaio, C.A.M. Sampaio, *Leucaena leucocephala* serine proteinase inhibitor: primary structure and action on blood coagulation, kinin release and rat paw edema, Biochim. Biophys. Acta 1477 (2000) 64–74.
[12] I. Cruz-Silva, A.J. Gozzo, V.A. Nunes, A.K. Carmona, A. Faljoni-Alario, M.L. Oliva, M.U. Sampaio, C.A. Sampaio, M.S. Araujo, A proteinase inhibitor from *Caesalpinia echinata* (pau-brasil) seeds for plasma kallikrein, plasmin and factor XIIa, Biol. Chem. 385 (2004) 1083–1086.
[13] E. Skrzydlewska, M. Sulkowska, M. Koda, S. Sulkowski, Proteolytic–antiproteolytic balance and its regulation in carcinogenesis, World J. Gastroenterol. 11 (2005) 1251–1266.
[14] D. Kuester, H. Lippert, A. Roessner, S. Krueger, The cathepsin family and their role in colorectal cancer, Pathol. Res. Pract. 204 (2008) 491–500.
[15] I. Podgorski, B.F. Sloane, Cathepsin B and its role(s) in cancer progression, Biochem. Soc. Symp. 70 (2003) 263–276.
[16] T. Nomura, N. Katunuma, Involvement of cathepsins in the invasion, metastasis and proliferation of cancer cells, J. Med. Invest. 52 (2005) 1–9.
[17] O. Vasiljeva, A. Papazoglou, A. Krüger, H. Brodoefel, M. Korovin, J. Deussing, N. Augustin, B.S. Nielsen, K. Almholt, M. Bogyo, C. Peters, T. Reinheckel, Tumor cell-derived and macrophage-derived cathepsin B promotes progression and lung metastasis of mammary cancer, Cancer Res. 66 (2006) 5242–5250.
[18] B. Goulet, L. Sansregret, L. Leduy, M. Bogyo, E. Weber, S.S. Chauhan, A. Nepveu, Increased expression and activity of nuclear cathepsin L in cancer cells suggests a novel mechanism of cell transformation, Mol. Cancer Res. 5 (2007) 899–907.
[19] S. Sullivan, M. Tosetto, D. Kevans, A. Coss, L. Wang, D. O'Donoghue, J. Hyland, K. Sheahan, H. Mulcahy, J. O'Sullivan, Localization of nuclear cathepsin L and its association with disease progression and poor outcome in colorectal cancer, Int. J. Cancer 125 (2009) 54–61.
[20] B. Cauwe, P.E. Van den Steen, G. Opdenakker, The biochemical, biological, and pathological kaleidoscope of cell surface substrates processed by matrix metalloproteinases, Crit. Rev. Biochem. Mol. Biol. 42 (2007) 113–185.
[21] J.W. van der Stappen, A.C. Williams, R.A. Maciewicz, C. Paraskeva, Activation of cathepsin B, secreted by a colorectal cancer cell line requires low pH and is mediated by cathepsin D, Int. J. Cancer 67 (1996) 547–554.
[22] M.A. Mohamed, S. Cunningham-Rundles, C.R. Dean, T.A. Hammad, M. Nesin, Levels of pro-inflammatory cytokines produced from cord blood in-vitro are pathogen dependent and increased in comparison to adult controls, Cytokine 39 (2007) 171–177.
[23] M.L. Oliva, D. Grisolia, M.U. Sampaio, C.A.M. Sampaio, Properties of highly purified human plasma kallikrein, Agents Actions 9 (1982) 52–57.
[24] C. Oliveira, L.A. Santana, A.K. Carmona, M.H. Cezari, M.U. Sampaio, C.A.M. Sampaio, M.L.V. Oliva, Structure of cruzipain/cruzain inhibitors isolated from *Bauhinia bauhinioides* seeds, Biol. Chem. 382 (2001) 847–852.
[25] M.L. Oliva, C.R. Mendes, E.M. Santomauro-Vaz, M.A. Juliano, R. Mentele, E.A. Auerswald, M.U. Sampaio, C.A. Sampaio, *Bauhinia bauhinioides* plasma kallikrein inhibitor: interaction with synthetic peptides and fluorogenic peptide substrates related to the reactive site sequence, Curr. Med. Chem. 8 (2001) 977–984.
[26] A.P.U. Araújo, D. Hansen, D.F. Vieira, C. Oliveira, L.A. Santana, L.M. Beltramini, C.A.M. Sampaio, M.U. Sampaio, M.L. Oliva, Kunitz type *Bauhinia* bauhinioides inhibitors devoid of disulfide bridges: isolation of the cDNAs, heterologous expression and structural studies, Biol. Chem. 386 (2005) 561–568.
[27] C.A. Sampaio, M.U. Sampaio, E.S. Prado, Active-site titration of horse urinary kallikrein, Hoppe Seyler's Z, Physiol. Chem. 365 (1984) 297–302.
[28] E. Gasteiger, A. Gattiker, C. Hoogland, I. Ivanyi, R.D. Appel, A. Bairoch, Expasy: the proteomics server for in depth protein knowledge and analysis, Nucleic Acids Res. 31 (2003) 3784–3788.
[29] N. Sreerama, R.W. Woody, Analysis of protein CD spectra: comparison of CONTIN, SELCON3, and CDSSTR methods in CDPro software, Biophys. J. 78 (2000) 1974.
[30] C.H. Fiske, Y. Subbarow, The colorimetric determination of phosphorus, J. Biol. Chem. 66 (1925) 375–400.
[31] M.L. Oliva, M.U. Sampaio, *Bauhinia* Kunitz-type proteinase inhibitors: structural characteristics and biological properties, Biol. Chem. 389 (2008) 1007–1013.
[32] J. Wu, J.T. Yang, C.S. Wu, Beta-II conformation of all-beta proteins can be distinguished from unordered form by circular dichroism, Anal. Biochem. 200 (1992) 359–364.
[33] S.Y. Venyaminov, J.T. Yang, Determination of protein secondary structure, in: G.D. Fasman (Ed.), Circular Dichroism and the Conformational Analysis of Biomolecules, Plenum Press, New York, 1996, pp. 69–108.

[34] R.W. Woody, A.K. Dunker, Aromatic and cystine side-chain circular dichroism in proteins, in: G.D. Fasman (Ed.), Circular Dichroism and the Conformational Analysis of Biomolecules, Plenum Press, New York, 1996, pp. 109–158.
[35] N. Sreerama, R.W. Woody, Computation and analysis of protein circular dichroism spectra, Methods Enzymol. 383 (2004) 318–351.
[36] D. Hansen, S. Macedo-Ribeiro, P. Verissimo, S. Yoo Im, M.U. Sampaio, M.L. Oliva, Crystal structure of a novel cysteinless plant Kunitz-type protease inhibitor, Biochem. Biophys. Res. Commun. 360 (2007) 735–740.
[37] M.V. Navarro, D.F. Vierira, R.A. Nagem, A.P. Araújo, M.L. Oliva, R.C. Garrat, Crystallization and preliminary X-ray analysis of a novel Kunitz-type kallikrein inhibitor from *Bauhinia bauhinioides*, Acta Crystallogr. Sect. F. Struct. Biol. Cryst. Commun. (2005) 910–913.
[38] H.T. Yu, W. Colucci, M.L. Maclaughlin, M.D. Barkley, Fluorescence quenching in indoles by excited-state proton transfer, J. Am. Chem. Soc. 114 (1992) 8449–8454.
[39] Y. Chen, M.D. Barkley, Toward understanding tryptophan fluorescence in proteins, Biochemistry 37 (1998) 9976–9982.
[40] A.S. Ladokhin, Fluorescence spectroscopy in peptide and protein analysis, in: R.A. Meyers (Ed.), Encyclopedia of Analytical Chemistry, 2000, pp. 5762–5779.
[41] T. Renné, J. Dedio, G. David, W. Müller-Ester, High molecular weight kininogen utilizes heparan sulfate proteoglycans for accumulation on endothelial cells, J. Biol. Chem. 275 (2000) 33688–33696.
[42] T. Renné, W. Müller-Ester, Cell surface-associated chondroitin sulfate proteoglycans bind contact phase factor H-kininogen, FEBS Lett. 500 (2001) 36–40.
[43] K.R. Melo, A. Gutierrez, F.D. Nascimento, M.K. Araújo, M.U. Sampaio, A.K. Carmona, Y.M. Coulson-Thomas, E.S. Trindade, H.B. Nader, I.L. Tersariol, G. Motta, Involvement of heparan sulfate proteoglycans in cellular uptake of high molecular weight kininogen, Biol. Chem. 390 (2009) 145–155.